Topology of the Retinal Cone NCKX2 Na/Ca−K Exchanger†

Tashi G. Kinjo, Robert T. Szerencsei, Robert J. Winkfein, KyeongJin Kang, and Paul P. M. Schnetkamp*

Department of Physiology & Biophysics, Faculty of Medicine, University of Calgary, 3330 Hospital Drive, N.W. Calgary, Alberta, Canada T2N 4N1

Received October 29, 2002; Revised Manuscript Received December 9, 2002

ABSTRACT: The Na/Ca−K exchanger (NCKX) is a polytopic membrane protein that plays a critical role in Ca^{2+} homeostasis in retinal rod and cone photoreceptors. The NCKX1 isoform is found in rods, while the NCKX2 isoform is found in cones, in retinal ganglion cells, and in various parts of the brain. The topology of the Na/Ca−K exchanger is thought to consist of two large hydrophilic loops and two sets of transmembrane spanning segments (TMs). The first large hydrophilic loop is located extracellularly at the N-terminus; the other is cytoplasmic and separates the two sets of TMs. The TMs consist of either five and five membrane spanning helices or five and six membrane spanning helices, depending upon the predictive algorithm used. Little specific information is yet available on the orientation of the various membrane spanning helices and the localization of the short loops connecting these helices. In this study, we have determined which of the connecting loops are exposed to the extracellular milieu using two different methods: accessibility of substituted cysteine residues and insertion of *N*-glycosylation sites. The two methods resulted in a consistent NCKX topology in which the two sets of TMs each contain five membrane spanning helices. Our new model places what was previously membrane spanning helix six in the cytoplasm, which places the C-terminus on the extracellular surface. Surprisingly, this NCKX topology model is different from the current NCX topology model with respect to the C-terminal three membrane helices.

The Na/Ca−K exchanger (NCKX)[1] utilizes both the inward Na^+ gradient and the outward K^+ gradient for the extrusion of Ca^{2+} across the plasma membrane. To date, three human NCKX isoforms have been cloned from retinal cDNA libraries: NCKX1 is found in rod photoreceptors (*1*); NCKX2 is found in retinal cone photoreceptors, retinal ganglion cells (*2*), and in various parts of the brain (*3*); while NCKX3 was shown to have a more broad expression pattern (*4*). NCKX paralogs have also been cloned from sea urchin (*5*), *Drosophila* (*6*), and *Caenorhabditis elegans* (*7*). Most of these cDNAs have been shown to result in potassium-dependent reverse Na/Ca−K exchange function when transfected into cells that lack endogenous Na/Ca(−K) exchange. Hydropathy analysis of the various NCKX sequences has shown a uniform pattern of two large hydrophilic loops and two sets transmembrane spanning segments (TM). The two large hydrophilic loops show little sequence similarity between different paralogs; they are found at the N-terminus, thought to be located in the extracellular space, and between the two TMs and thought to be located in the cytosol. The two sets of TMs are predicted to consist of five and six, or five and five membrane spanning helices, respectively, dependent on the predictive algorithm used (Figure 1). The membrane spanning helices and their short connecting loops (<24 residues) are well-conserved between the different NCKX genes, especially in two short stretches of about 40−60 residues each, one in each TM. These so-called α 1 and α 2 repeats are thought to have arisen from an ancient gene duplication event (*8*) and contain the only sequence elements that show sequence similarity between members of the NCKX and NCX (Na/Ca exchanger) gene families.

It has been shown that the two hydrophilic loops can be removed from NCKX1 without affecting Na/Ca−K exchange transport function (*7*, *9*, *10*). This suggests that they do not contain any transmembrane spanning segments important for NCKX function (except for the putative cleavable signal sequence at the far N-terminus) and that removal did not change the NCKX topology. In this study, we have examined the orientation of all the proposed transmembrane spanning helices in the human retinal cone NCKX2 using two different methods. Human retinal cone NCKX2 was chosen as it is one of the best expressing NCKX clones we generated and since it contains only a single endogenous glycosylation site. First, we eliminated the single endogenous glycosylation site, and subsequently, we inserted a glycosylation site into each of the predicted short connecting loops and looked for glycosylation of these sites to indicate an extracellular localization. Second, we used a cysteine scanning analysis in which a large number of residues were replaced individually by cysteine residues, and we examined whether NCKX

† This work was supported by an operating grant from the Canadian Institutes for Health Research to P.P.M.S. P.P.M.S. is a scientist of the Alberta Heritage Foundation for Medical Research, T.G.K. is a recipient of a studentship from the Alberta Heritage Foundation for Medical Research, and K.J.K. is a recipient of a studentship from the Canadian Foundation Fighting Blindness.

* To whom correspondence should be addressed. Tel.: (403) 220-5448. Fax (403) 283-8731. E-mail: pschnetk@ucalgary.ca.

[1] Abbreviations used: DMF, dimethyl formamide; PNGase F, peptide:*N*-glycosidase F; MTSET, [2-(trimethylammonium) ethyl] methanethiosulfonate bromide; MTSEA, (2-aminoethyl)methanethiosulfonate hydrobromide; NCKX, Na/Ca−K exchanger; NCX, Na/Ca exchanger; MW, molecular weight; TM, transmembrane spanning segment.

10.1021/bi0270788 CCC: $25.00
Published on Web 02/04/2003

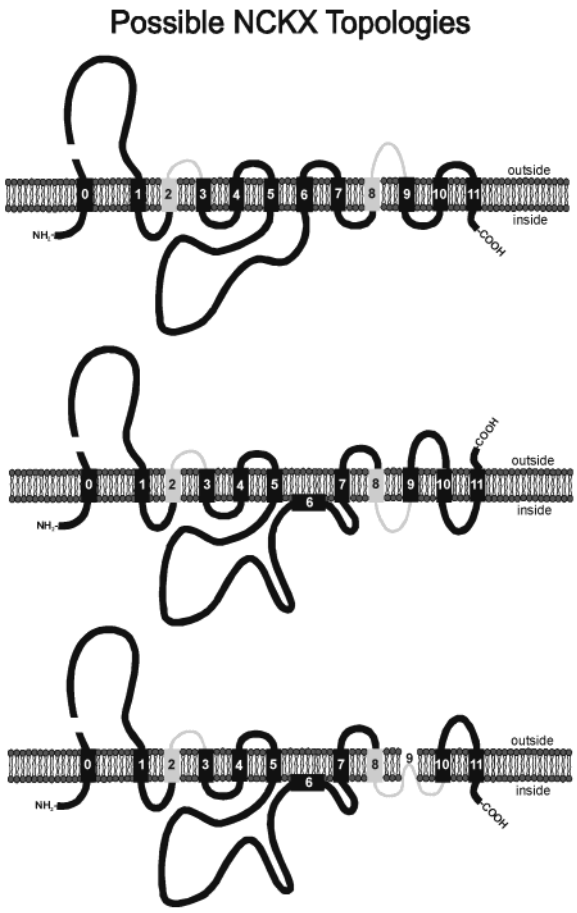

FIGURE 1: Different NCKX topology models. Top: topology based on Kyte−Doolittle analysis. Middle: topology based on the TmHMM algoritm (http://www.cbs.dtu.dk/services/TMHMM-2.0/). Bottom: current topology model of NCX1. The α repeats are indicated in light gray. The cut in the sequence just above the H0 segment indicates cleavage of the putative signal peptide to yield the mature NCKX protein.

function had gained a sensitivity toward the impermeant cysteine reagent MTSET. Our results are consistent with a model in which each of the sets of TM's contains five membrane spanning helices, and which places the C-terminus on the extracellular surface. This model is different from the current topology model of the NCX1 Na/Ca exchanger (*11*, *12*).

EXPERIMENTAL PROCEDURES

Generation of Spacer Containing Clones. A spacer consisting of 41 amino acids (SHVDHISAETEMEGEGNETGECTGSYYCKKGVILPIWEDEP) taken from the N-terminus of the sodium−calcium exchanger (NCX1) was inserted individually into all the short loops connecting the putative membrane spanning α helices of the human retinal cone NCKX2. Mutant constructs were made in the short splice variant of the human retinal cone NCKX2 cDNA (AAF25811). This clone contains the human c-Myc tag (EQKLISEEDL) inserted at the BstE II site between bases 241−242 (at amino acid residue 81) of the human cone NCKX2 sequence. In all spacer containing clones, the wild-type *N*-glycosylation site (asparagine at amino acid residue 111) was mutated to an aspartate using cassette mutagenesis with upper and lower primers upstream and downstream of the restriction sites used to clone the fragment. Cassette mutagenesis was used to introduce Xho I sites between the different membrane spanning α helices of the human cone NCKX2. The introduced Xho I site was then used to insert the spacer as indicated in Table 1. The spacer itself was PCR amplified using primers that introduced flanking Xho I sites. All PCR generated fragments were thoroughly sequenced after insertion to ensure no unwanted mutations were generated through PCR errors. Plasmid DNAs were prepared using the EndoFree Plasmid Maxi Kit system from Qiagen (Mississauga, Ontario, Canada).

Transient Expression of Human Mutant and Myc-Tagged Cone NCKX2 cDNAs in Insect Cells. A lepidoteran insect cell expression system was used for transient transfection of BTI-TN-5B1-4 (High Five; Invitrogen) insect cells with the various mutant human cone NCKX2 cDNAs as described previously (*7*). High Five cells were subcultured at 28 °C in IPL-41 insect medium (Life Technologies, Burlington, Ontario, Canada) supplemented with 0.35 g/L $NaHCO_3$, 2.6 g/L tryptose phosphate, 9.0 g/L sucrose, 0.069 mg/L $ZnSO_4 \cdot 7H_2O$, 7.59 mg/L $AIK(SO_4)_2 \cdot 12H_2O$, 10% heat-inactivated fetal bovine serum (GibcoBRL), and penicillin−streptomycin−fungizone (GibcoBRL).

Measurement of $^{45}Ca^{2+}$ Uptake via Na/Ca−K Exchange and MTSET Treatment. Potassium-dependent Ca^{2+} uptake was measured in sodium-loaded High Five cells transiently transfected with the various mutant human cone NCKX2 cDNAs as previously described (*7*). Incubation of cells with MTSET (Biotium, Hayward, California) or DMF (as a vehicle control) took place prior to the sodium loading protocol. Transiently transfected High Five cells were collected 48 h post transfection and washed twice with 150 mM NaCl, 20 mM Hepes, 80 mM sucrose, and 200 μM EDTA, pH 7.4. About two million cells were incubated for 5 min at room temperature with 2 mM MTSET in this medium in a total volume of 500 μL. MTSET treatment and sodium loading on cells expressing different mutant NCKX proteins was carried out in a staggered way to control strictly the amount of time elapsed between the end of the sodium loading protocol and the start of the $^{45}Ca^{2+}$ uptake experiment. Background $^{45}Ca^{2+}$ uptake was monitored by using untransfected cells or cells transfected with empty vector.

Deglycosylation of Spacer Containing Human Cone NCKX2 Mutant Protein. High Five cells transiently transfected with the various spacer containing human cone NCKX2 cDNAs were treated with the glycosidase PNGase F (New England Biolabs). Cells were collected 48 h post-transfection and washed two times with 150 mM NaCl, 20 mM Hepes, 80 mM sucrose, and 200 μM EDTA, pH 7.4. The cells were then incubated for 20 min in ice-cold RIPA buffer containing 140 mM NaCl, 25 mM Tris (pH 7.5), 1% Triton X-100, 0.5% sodium deoxycholate, 0.1 mM EDTA, and a protease inhibitor tablet (Roche Molecular Biochemicals). The suspension was spun at 20 000*g* for 5 min, and the supernatant was collected. Protein concentration of the supernatant was determined using the Bio-Rad protein assay (Biorad Laboratories, Mississauga, Ontario, Canada). The extract was then denatured by adding 0.5% SDS and 1% β-mercaptoethanol and incubated at 37 °C for 10 min. NP-40 and Na_2PO_4 were added to each sample to a final concentration of 1% and 50 mM, respectively. PNGase F was then added to the treated samples to a final concentration of 2 units/μL. All samples were then incubated at 37 °C for

Table 1[a]

clone	human cone NCKX AA sequence	AA sequence flanking the spacer
H1−H2	157 FVPSLTVITE 166	FVPSR**SHV...WEDEP**GSSTVITE
H2−H3	196 VFIAHSNVGI 205	VFIAR**GSHV...WEDEPRG**NVGI
H3−H4	329 EILNLTWWPL 238	EILNLE**SHV...WEDE**LEWWPL
H4−H5	263 WWESLLLLTA 272	WWDSR**SHV...WEDEP**GSRSLLLLTA
H6−H7	491 RKPSSRKFFP 500	RKPSSR**SHV...WEDEP**GSRKFFP
H7−H8	523 QVGETIGISE 532	QVLE**SHV...WEDE**LETIGISE
H8−H9	557 RKGLGDMAVS 566	RKGLE**SHV...WEDE**LEGDMAVS
H9−H10	591 HRFQPVAVSS 600	HRFQLE**SHV...WEDE**LEAVSS
H10−H11	626 WRMNKILGFI 635	WRMNSR**SHV...WEDEP**GSRKILGFI
C-terminus	653 RILTCPVSI@ 661	RILE**SHV...WEDE**LELTCPVSI@

[a] Bold lettering indicates spacer amino acids. Underlined amino acids indicate changes to the wild-type amino acid sequence.

1.5 h. Sample buffer was added, and samples were subjected to gel electrophoresis in an 8% Laemmli gel.

RESULTS

Figure 1 illustrates three different candidate topology models for the NCKX protein based on predictive algorithms and based on the current topology model of the Na/Ca exchanger. Kyte−Doolittle analysis predicts a 1 plus 5 plus 6 arrangement of TM α helices (labeled H0 through H11) for NCKX (*3*, *13*, *14*): H0 is thought to represent a cleaved signal sequence, and the C-terminus is located intracellularly (Figure 1, top panel). More recent algorithms such as TmHMM (*15*) (http://www.cbs.dtu.dk/services/TMHMM-2.0/) predict a 1 plus 5 plus 5 arrangement of TM α helices for both NCKX1 and NCKX2: H0 is again predicted to represent a cleaved signal sequence, H6 is not placed in the membrane, and the C-terminus is located extracellularly (Figure 1, middle panel). Compared to the Kyte−Doolittle topology, the H6 segment is not predicted to be a transmembrane helix; H6 contains significant hydrophobicity, and 13 out of 21 residues are conserved between rod NCKX1 and cone/brain NCKX2. The predictive algorithms yield very similar topologies for NCX1 as illustrated for NCKX1 or NCKX2 in the top two panels of Figure 1. However, experimental data currently favor a NCX1 topology consisting of a 1 plus 5 plus 4 arrangement (Figure 1, bottom panel): H0 is a cleavable signal sequence, H6 is not within the membrane, while H9 forms a re-entrant loop that places the C-terminus intracellularly (*11*, *12*). Elsewhere, we have shown that H0 can be (partially) cleaved from both NCKX1 and NCKX2 expressed in either insect cell lines (High Five) or in mammalian cell lines (HEK293 cells) (Kang, K-.J., and Schnetkamp, P. P. M., in preparation). To distinguish between the three topology models illustrated in Figure 1, we have used two different methods to examine the extracellular localization of the various short connecting loops in the two sets of TMs.

Insertion of Glycosylation Sites. Introduction of *N*-glycosylation sites into the loops of polytopic membrane proteins is a well-established method to detect extracellular connecting loops. The human cone NCKX2 contains a single consensus *N*-glycosylation site at N111. The single site mutant N111D was made, and treatment of this NCKX2 mutant with glycosidases did not result in any molecular weight shift indicating that no further endogenous *N*-glycosylation sites were present, whereas a significant shift in molecular weight was observed for the wild-type NCKX2 (Figure 2, left panel). Human NCKX2 expressed in either insect cells or in

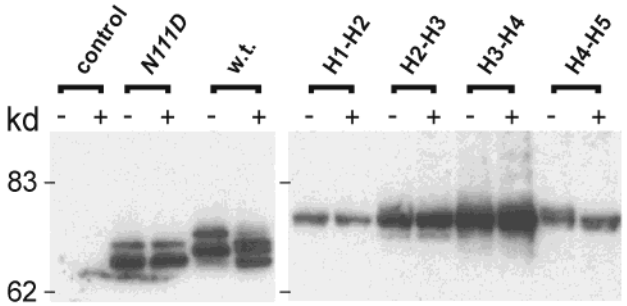

FIGURE 2: Western blot analysis of wild-type NCKX2 and various glycosylation site mutants in the first set of TMs. Expressed NCKX proteins were detected with the human Myc tag antibody; the Myc tag was inserted in the N-terminal external loop of all our NCKX2 constructs. The white dashes are a visual aid to align bands. Untreated samples are indicated by the minus sign; samples treated with PNGase F are identified by the plus sign. The nomenclature of the various spacer inserts is according to Figure 1.

HEK293 cells consistently ran as a doublet on SDS−PAGE, representing full-length NCKX2 (upper band) and NCKX2 from which H0 was cleaved (Kang, K-.J., and Schnetkamp, P. P. M., in preparation). We have used the N111D mutant for all further constructs in which *N*-glycosylation sites were introduced in various parts of the NCKX2 sequence. It has been shown for other membrane proteins that extracellular connecting loops must be at least 25 residues long to show *N*-glycosylation of an appropriate acceptor site (*16*). Unfortunately, the connecting loops of the TM segments in NCKX are too short to meet this criterium. Therefore, we inserted a 41 amino acid spacer into all nine possible connecting loops as well as at the C-terminus. The spacer (SHVDHISAETEMEGEG*N*ETGECTGSYYCKKGVILPIWEDEP) is part of the extracellular loop of the bovine heart NCX1 and contains a single *N*-glycosylation site (in bold italics) as well as the epitope for the 6H2 monoclonal antibody. We have used this sequence as a spacer in several other NCKX constructs from which we concluded that it does not impart any novel functional or inhibitory properties on NCKX.

Figure 2 (right panel) illustrates the effect of PNGase F (peptide:*N*-glycosidase F) treatment on the apparent molecular weight (MW) of the different mutant NCKX2 proteins representing the spacer inserted into each of the short connecting loops of the first set of TMs. These constructs ran at a slightly higher MW because of the added mass of the spacer. As observed for wild-type NCKX2, the spacer inserts generally showed two bands on SDS−PAGE, although in some cases the lower band was rather faint, and the separation between the two bands was not always as clear. For this reason, we focused here on the observation

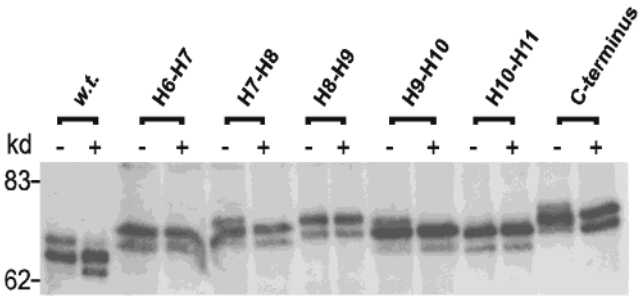

FIGURE 3: Western blot analysis of wild-type NCKX2 and various glycosylation site mutants in the second set of TMs. Expressed NCKX proteins were detected with the human Myc tag antibody; the Myc tag was inserted in the N-terminal external loop of all our NCKX2 constructs. The white dashes are a visual aid to align bands. Untreated samples are indicated by the minus sign; samples treated with PNGase F are identified by the plus sign. The nomenclature of the various spacer inserts is according to Figure 1.

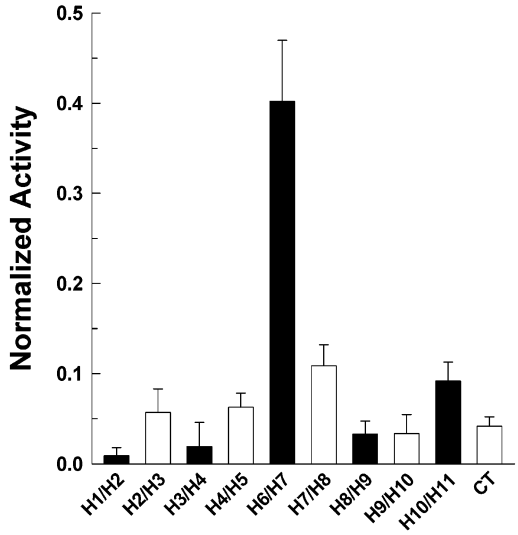

FIGURE 4: Functional activity of the different glycosylation site mutants. NCKX function was measured as the difference of $^{45}Ca^{2+}$ uptake via reverse Na/Ca−K exchange in high K^+ medium and that in high Na^+ medium as described in detail elsewhere (*7*). $^{45}Ca^{2+}$ uptake in high Na^+ medium was very similar to that observed in cells transfected with empty vector. The data were normalized to uptake observed in cells transfected with wild-type NCKX2. Average ± standard error of the mean are shown for five independent transfection experiments. The nomenclature of the various spacer inserts is according to Figure 1. Temperature: 25 °C.

that PNGase F treatment resulted in a consistent removal of a higher MW band in some of the constructs representing the spacer inserts. Thus, PNGase F treatment resulted in a consistent lowering of the MW of the H4−H5 spacer construct suggesting the H4−H5 spacer was glycosylated and located extracellularly, whereas the H1−H2 and H3−H4 never showed a shift upon PNGase F treatment, consistent with an intracellular localization. A small shift was sometimes observed when the spacer was introduced into the H2−H3 linker. Figure 3 illustrates the effect of PNGase F treatment on the MW of the different mutant NCKX2 proteins representing the spacer inserted into each of the short connecting loops of the second set of TMs. All the spacer inserts resulted in mutant NCKX2 proteins that in this experiment ran as doublets in PNGase F treated samples. In untreated samples, however, the H7−H8 and H9−H10 spacer inserts as well as the insert at the C-terminus yielded mutant NCKX2 proteins that showed an additional upper band that was removed by PNGase F treatment. This suggests that these spacers could, at least in part, be *N*-glycosylated when provided with a suitable glycosylation site, implying an extracellular localization for the H7−H8 and H9−H10 linkers as well as for the C-terminus. In contrast, no effect of PNGase F treatment was observed in mutant NCKX2 proteins representing the H6−H7, H8−H9, and H10−H11 spacers, consistent with an intracellular localization. The increase in mobility observed after PNGase F treatment observed for the spacer inserts was smaller than observed for the wild-type human NCKX2, perhaps because the close proximity to the membrane surface for the glycosylation sites inserted into the linkers impeded access by glycosidases. The pattern shown in Figures 2 and 3 was consistently observed in at least four independent experiments in which the various spacer NCKX2 constructs were expressed in High Five cells; a similar pattern of *N*-glycosylation was observed when the spacer constructs were expressed in HEK293 cells (results not shown). Of the three topology models shown in Figure 1, the glycosylation results illustrated in Figures 2 and 3 are only consistent with the 1 plus 5 plus 5 arrangement of TM helices (Figure 1, middle panel).

The above spacer inserts are placed in highly conserved parts of the NCKX2 sequence, which could compromise NCKX function. Figure 4 illustrates a quantitative assessment of NCKX function of the mutant NCKX2 proteins obtained with the various spacer inserts; mutant NCKX function is normalized to the wild-type human cone NCKX2 activity. The H6−H7 spacer insert showed robust reverse Na/Ca−K exchange function, close to wild-type NCKX function when allowance is made for somewhat reduced protein expression levels. In contrast, all other spacer inserts resulted in mutant NCKX2 proteins with strongly reduced transport function. The mutant NCKX2 proteins containing either the H2−H3, H4−H5, H7−H8, or the H10−H11 spacer inserts showed significant residual NCKX function, whereas mutant NCKX2 proteins containing the H1−H2, H3−H4, H8−H9, H9−H10 inserts, and the insert at the C-terminus showed very little NCKX function.

Cysteine Scanning Mutagenesis and MTSET Accessibility. Cysteine susceptibility is often tested with the impermeant MTSET reagent as well as with the membrane permeant MTSEA reagent, the latter to modify cysteine residues accessible only from the intracellular space. However, MTSEA had strong effects on intracellular Ca^{2+} handling, which precluded its use in our functional NCKX assays (data not shown). Therefore, we limited ourselves here to analyze cysteine susceptibility to the impermeant MTSET and address accessibility to the extracellular milieu. We tested the effect of MTSET on ^{45}Ca uptake for NCKX2 proteins representing a total of 49 cysteine mutants covering all the linkers. In six mutants, MTSET was found to lead to a consistent and significant inhibition (>40%) of NCKX2 function as measured by ^{45}Ca uptake via reverse Na/Ca−K exchange (Figure 5, top panel). G195 and V196 are located in H2, close to the surface near the H2−H3 linker; W519 is located in H7 close to the H7−H8 linker, while G536 and L540 are located in H8 close to the H7−H8 linker. Finally, L603 is located in H10, close to the H9−H10 linker. These results show that the H2−H3 and H7−H8 linkers are exposed to the extracellular milieu. As a consequence, the α 1 and α 2 repeats

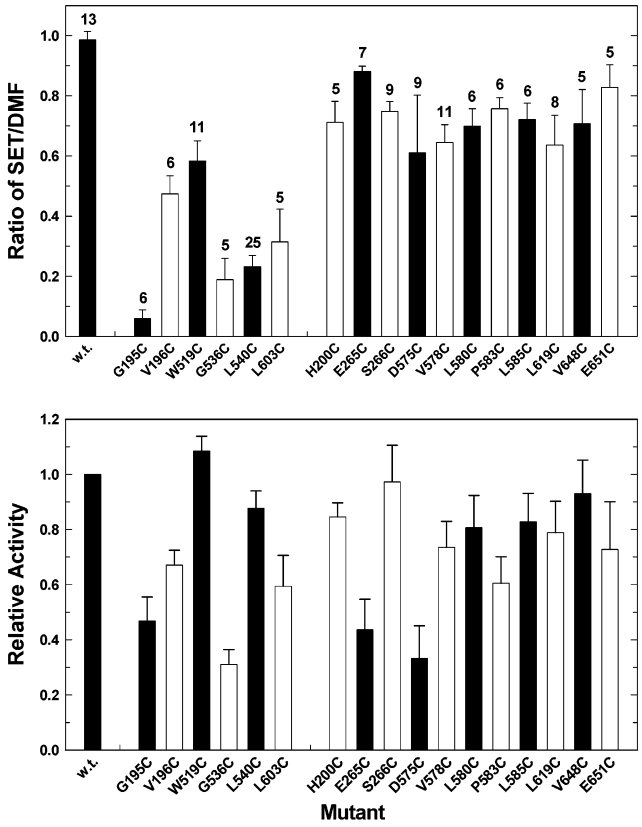

FIGURE 5: Effect of MTSET on NCKX function in insect cells expressing different cysteine mutants. $^{45}Ca^{2+}$ uptake via reverse Na/Ca−K exchange was measured in high K^+ medium in cells expressing the different NCKX2 (mutant) proteins with or without 2 mM MTSET present. Background $^{45}Ca^{2+}$ uptake observed in untransfected cells or in cells transfected with empty vector was subtracted, and the ratio of $^{45}Ca^{2+}$ uptake in the presence of MTSET and $^{45}Ca^{2+}$ uptake in the absence of MTSET was calculated. Average values of this ratio with standard error of the mean are presented for the indicated number of experiments. The lower panel illustrates the functional activity of these mutants in the absence of MTSET and normalized to wild-type NCKX2 activity. Temperature: 25 °C.

are in opposite orientation, consistent with the 1 plus 5 plus 5 topology or the topology proposed for NCX1 (see Figure 1). An extracellular location of L603 near the H9−H10 linker is consistent with the glycosylation results (Figure 2) and would appear to be consistent only with the 1 plus 5 plus 5 topology. A further 11 cysteine substitutions showed more modest inhibitory effects (20−30% inhibition) of MTSET on ^{45}Ca uptake via reverse Na/Ca−K exchange (Figure 5, top panel), whereas an additional 32 cysteine mutants were tested and found to have no consistent MTSET-dependent inhibitory effects on NCKX2 function. For all cysteine mutants, tested transport activity was at least 30% of wild-type NCKX2 activity (Figure 5, bottom panel). Figure 6 illustrates the location of all 16 cysteine residues that appeared to impart MTSET sensitivity on NCKX2-mediated ^{45}Ca uptake. With the exception of L619, these results are consistent with the 1 plus 5 plus 5 topology suggested by the glycosylation experiments.

DISCUSSION

The retinal rod and cone NCKX1 and NCKX2 Na/Ca−K exchangers are polytopic membrane proteins that, on the basis of predictive algorithms, are thought to consist of a cleavable signal peptide and sets of five plus five or five plus six transmembrane spanning helices separated by a large hydrophilic loop (Figure 1). In earlier studies, normal Na/Ca−K exchange function was observed for bovine rod NCKX1 in which the two large hydrophilic loops were removed, either by proteolysis (*9*) or by mutagenesis (*7*, *10*). This is consistent with the general nature of the topological models illustrated in Figure 1. In this study, we used two different approaches to test the localization of the short connecting loops in the two sets of TMs of the retinal cone NCKX2: (1) insertion of a spacer containing an *N*-glycosylation site into all the possible linkers; and (2) accessibility of substituted cysteine residues to the reagent MTSET.

Analysis of Endogenous and Inserted Glycosylation Sites. Removal of the putative single glycosylation site N111D in human cone NCKX2 led to a lowering of the MW of the expressed protein and eliminated a MW shift induced by glycosidases (Figure 2). This demonstrates that N111 is indeed the only endogenous glycosylation site used by human NCKX2 in heterologous systems (High Five cells and HEK293 cells), and it confirms the extracellular localization of the N-terminal hydrophilic loop of NCKX2. We inserted a spacer containing a single *N*-glycosylation site individually into all the short loops connecting the different putative TM helices and at the C-terminus. This was carried out in the N111D mutant that lacks an endogenous glycosylation site. The effect of PNGase F on the mobility of the different spacer insertion constructs, illustrated in Figures 2 and 3, gave a consistent and alternating pattern of linkers that display (partially) glycosylated bands of lower mobility, followed or preceded by a linker that showed no change after glycosidase treatment. This alternating pattern seems to rule out the presence of re-entrant loop structures as the connecting loops are too short to accommodate both a re-entrant loop and a transmembrane spanning helix. Of the three topology models considered, the 1 plus 5 plus 5 topology and the C-terminus located extracellularly is the only one consistent with this pattern (Figure 1). As the spacers are inserted in highly conserved parts of the NCKX sequence, a concern is that the inserts may negatively affect function, and this was indeed observed with most inserts showing significantly reduced NCKX function (Figure 4).

MTSET Accessibility of Substituted Cysteine Residues. To obtain further information on the NCKX topology, we used MTSET accessibility of substituted cysteine residues as illustrated in Figure 5. The current topology model of NCX1 was obtained largely through application of this methodology (*11*, *12*). Individual cysteine substitutions were introduced in 49 residues of the wild-type NCKX2, and the effect of MTSET on NCKX function was examined for each mutant. The results are illustrated in Figure 5 and are superimposed on the 1 plus 5 plus 5 topology suggested by the glycosylation experiments (Figure 6). MTSET had no effect on wild-type NCKX function and the majority of the above 49 individual cysteine mutants. Strong MTSET sensitivity was imparted on NCKX function by the cysteine substitutions of G195 and V196, G536 and L540, and L603, respectively, consistent with the extracellular localization of the H2−H3, H7−H8, and H9−H10 linkers. This confirms for NCKX the opposite orientation of the α 1 and α 2 repeats, similar as observed for the NCX1 topology (*11*, *12*). The strongest

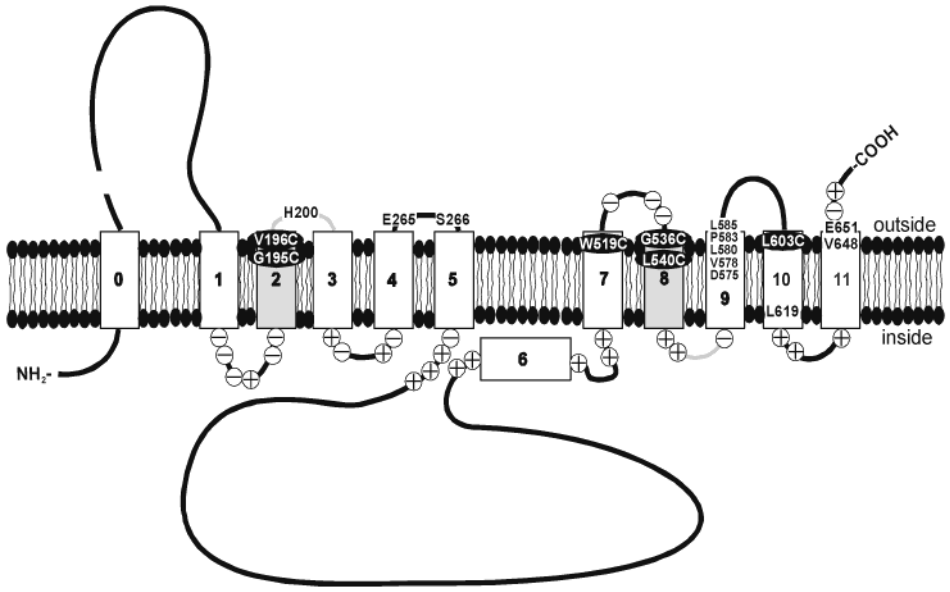

FIGURE 6: Proposed NCKX topology. The results of the topology experiments reported here are summarized. The 1 plus 5 plus 5 topology illustrated here is based on the results of the glycosylation site insert experiments shown in Figures 2 and 3. MTSET accessible residues are indicated. Residues on a black oval background were strongly affected by MTSET (>40% inhibition), while residues in black lettering were modestly affected by MTSET (~20% inhibition). Charged residues in the short connecting loops are indicated as well. The cut in the sequence just above the H0 segment indicates cleavage of the putative signal peptide to yield the mature NCKX protein.

MTSET inhibition was observed for residues at the extracellular surface of H2 (G195 and 196) and H8 (G536 and L540), respectively. The importance of H2 and H8 for NCKX function was recently reported in another study, in which we determined that H2 and H8 contain acidic and hydroxyl containing residues critical to NCKX function (*17*). Thus, residues at the extracellular surface of both helix 2 and 8 appear to be located near the access pathway to these critical residues in the membrane interior. Placing a bulky and positively charged group on a residue in the access pathway could strongly impede access of cations for both steric and electrostatic reasons and cause the observed inhibition. The results of the MTSET experiments discussed so far encompassing H0 through H8 are consistent with results obtained with NCX1 (*11, 12*), suggesting a very similar topology for NCKX and NCX1 up to H8.

Topology of the C-Terminal Part: Comparison with NCX Topology. NCKX exchanges cations across the membrane from the intracellular space to the extracellular milieu and vice versa. The implication is that some key residues involved in cation binding and cation transport are likely to be exposed to both intracellular and extracellular milieu, dependent on the conformational state of the protein (i.e., inward-facing or outward-facing). This may be reflected by MTSET accessibility to residues located well within the membrane, as has been shown for the two re-entrant loop structures of NCX1 (*15*). In the case of NCKX2, a string of residues in H9 were affected by MTSET (albeit modestly), of which residues D575 and V578 are thought to be located well within the membrane helix H9. In contrast, very few residues in H9 of NCX1 were found to be accessible to external MTSET, whereas a large number of residues were accessible to internal MTSET (*15*), consistent with a re-entrant loop structure. This places the H9−H10 linker of NCX1 at the intracellular surface. We obtained an apparently different result for NCKX as L603C, located in helix 10 close to the H9−H10 linker, was strongly inhibited by MTSET, consistent with localization close to the extracellular surface. It is not impossible that L603 would be a re-entrant loop residue closest to the opposite membrane surface and accessible to MTSET, something similar to residues N842 and I847 in NCX1 (*15*). An important aspect to consider in interpreting the MTSET results is the interfacial borders of the proposed TM helices. For NCKX, we were guided in our placement of the borders of the TM α helices by the presence of small clusters of charged residues in most of the putative connecting loops; these charged residues are indicated in Figure 6.

With the exception of the effect of MTSET on the L619C mutant (Figures 5 and 6), all our results are consistent with the 1 plus 5 plus 5 topology (Figures 1 and 6), although no strong MTSET results were obtained for the C-terminus. This topology is different from that currently considered for the heart NCX1 Na/Ca exchanger, based on extensive data pertaining to accessibility of substituted cysteine residues (*11, 12, 15*). In this study, we show for NCKX that helix 6 is not a transmembrane spanning helix and that the two α repeats have an opposite orientation, similar to what has been shown before for NCX. This suggests a very similar overall topology for both NCX and NCKX, despite the fact that the sequence similarity is limited to the two α repeats only. The glycosylation data of Figures 2 and 3 show a very simple and internally consistent pattern, but some caution should be exercised as quantitative analysis shows that most of these glycoylsation site mutants show NCKX function but at a strongly reduced level as compared to wild-type NCKX2. It is perhaps appropriate to quote from the Iwamoto et al. (*15*): "The data suggest that the α 2 repeat and its C-terminal neighboring region contain a complex membrane loop structure. At the present, we have little information about the detailed structure of these regions, including the relative location of residues". Thus, although the experiments reported here mostly support the topology illustrated in Figure 6, which places the C-terminus on the outside and is

different from the currently considered NCX topology, further work is needed to confirm the topology of the C-terminal part of NCXK.

REFERENCES

1. Tucker, J. E., Winkfein, R. J., Cooper, C. B., and Schnetkamp, P. P. M. (1998) *IOVS 39*, 435−440.
2. Prinsen, C. F. M., Szerencsei, R. T., and Schnetkamp, P. P. M. (2000) *J. Neurosci. 20*, 1424−1434.
3. Tsoi, M., Rhee, K.-H., Bungard, D., Li, X. B., Lee, S.-L., Auer, R. N., and Lytton, J. (1998) *J. Biol. Chem. 273*, 4155−4162.
4. Kraev, A., Quednau, B. D., Leach, S., Li, X. F., Dong, H., Winkfein, R. J., Perizzolo, M., Cai, X., Yang, R., Philipson, K. D., and Lytton, J. (2001) *J. Biol. Chem. 276*, 23161−23172.
5. Su, Y. H., and Vacquier, V. D. (2002) *Proc. Natl. Acad. Sci. U.S.A. 99*, 6743−6748.
6. Haug-Collet, K., Pearson, B., Park, S., Webel, S., Szerencsei, R. T., Winkfein, R. J., Schnetkamp, P. P. M., and Colley, N. J. (1999) *J. Cell Biol. 147*, 659−669.
7. Szerencsei, R. T., Tucker, J. E., Cooper, C. B., Winkfein, R. J., Farrell, P. J., Iatrou, K., and Schnetkamp, P. P. M. (2000) *J. Biol. Chem. 275*, 669−676.
8. Schwarz, E. M., and Benzer, S. (1997) *Proc. Natl. Acad. Sci. U.S.A. 94*, 10249−10254.
9. Kim, T. S. Y., Reid, D. M., and Molday, R. S. (1998) *J. Biol. Chem. 273*, 16561−16567.
10. Szerencsei, R. T., Prinsen, C. F. M., and Schnetkamp, P. P. M. (2001) *Biochemistry 40*, 6009−6015.
11. Nicoll, D. A., Ottolia, M., Lu, L., Lu, Y., and Philipson, K. D. (1999) *J. Biol. Chem. 274*, 910−917.
12. Iwamoto, T., Nakamura, T. Y., Pan, Y., Uehara, A., Imanaga, I., and Shigekawa, M. (1999) *FEBS Lett. 446*, 264−268.
13. Reiländer, H., Achilles, A., Friedel, U., Maul, G., Lottspeich, F., and Cook, N. J. (1992) *EMBO J. 11*, 1689−1695.
14. Cooper, C. B., Winkfein, R. J., Szerencsei, R. T., and Schnetkamp, P. P. M. (1999) *Biochemistry 38*, 6276−6283.
15. Iwamoto, T., Uehara, A., Imanaga, I., and Shigekawa, M. (2000) *J. Biol. Chem. 275*, 38571−38580.
16. Popov, M., Tam, L. Y., Li, J., and Reithmeier, R. A. (1997) *J. Biol. Chem. 272*, 18325−18332.
17. Winkfein, R. J., Szerencsei, R. T., Kinjo, T. G., Kang, K.-J., Perizzolo, M., Eisner, L., and Schnetkamp, P. P. M. (2003) *Biochemistry 42*, 543−552.

BI0270788